Conflicting phylogenetic signals in plastomes of the tribe Laureae (Lauraceae)

Tian-Wen Xiao [1, 2], **Yong Xu** [1, 2], **Lu Jin** [1, 2], **Tong-Jian Liu** [1], **Haifei Yan** [1], **Xuejun Ge** [Corresp. 1]

[1] Guangdong Provincial Key Laboratory of Applied Botany and Key Laboratory of Plant Resources Conservation and Sustainable Utilization, South China Botanical Garden, Chinese Academy of Sciences, Guangzhou, Guangdong, People's Republic of China

[2] University of Chinese Academy of Sciences, Beijing, People's Republic of China

Corresponding Author: Xuejun Ge
Email address: xjge@scbg.ac.cn

Background. Gene tree discordance is common in phylogenetic analyses. Many phylogenetic studies have excluded non-coding regions of the plastome without evaluating their impact on tree topology. In general, plastid loci have often been treated as a single unit, and tree discordance among these loci has seldom been examined. Using samples of Laureae (Lauraceae) plastomes, we explored plastome variation among the tribe, examined the influence of non-coding regions on tree topology, and quantified intra-plastome conflict.

Results. We found that the plastomes of Laureae have low inter-specific variation and are highly similar in structure, size, and gene content. Laureae was divided into three groups, subclades I, II and III. The inclusion of non-coding regions changed the phylogenetic relationship among the three subclades. Topologies based on coding and non-coding regions were largely congruent except for the relationship among subclades I, II and III. By measuring the distribution of phylogenetic signal across loci that supported different topologies, we found that nine loci (two coding regions, two introns and five intergenic spacers) played a critical role at the contentious node.

Conclusions. Our results suggest that subclade III and subclade II are successively sister to subclade I. Conflicting phylogenetic signals exist between coding and non-coding regions of Laureae plastomes. Our study highlights the importance of evaluating the influence of non-coding regions on tree topology and emphasizes the necessity of examining discordance among different plastid loci in phylogenetic studies.

Conflicting phylogenetic signals in plastomes of the tribe Laureae (Lauraceae)

Tian-Wen Xiao[1,2], Yong Xu[1,2], Lu Jin[1,2], Tong-Jian Liu[1], Hai-Fei Yan[1], Xue-Jun Ge[1]

[1] Guangdong Provincial Key Laboratory of Applied Botany and Key Laboratory of Plant Resources Conservation and Sustainable Utilization, South China Botanical Garden, Chinese Academy of Sciences, Guangzhou, Guangdong, China.

[2] University of Chinese Academy of Sciences, Beijing, China

Corresponding author:

Xue-Jun Ge

Email address: xjge@scbg.ac.cn

ORCID:

Xue-Jun Ge: orcid.org/0000-0002-5008-9475

Tian-Wen Xiao: orcid.org/0000-0002-7479-7089

Abstract

Background. Gene tree discordance is common in phylogenetic analyses. Many phylogenetic studies have excluded non-coding regions of the plastome without evaluating their impact on tree topology. In general, plastid loci have often been treated as a single unit, and tree discordance among these loci has seldom been examined. Using samples of Laureae (Lauraceae) plastomes, we explored plastome variation among the tribe, examined the influence of non-coding regions on tree topology, and quantified intra-plastome conflict.

Results. We found that the plastomes of Laureae have low inter-specific variation and are highly similar in structure, size, and gene content. Laureae was divided into three groups, subclades I, II and III. The inclusion of non-coding regions changed the phylogenetic relationship among the three subclades. Topologies based on coding and non-coding regions were largely congruent except for the relationship among subclades I, II and III. By measuring the distribution of phylogenetic signal across loci that supported different topologies, we found that nine loci (two coding regions, two introns and five intergenic spacers) played a critical role at the contentious node.

Conclusions. Our results suggest that subclade III and subclade II are successively sister to subclade I. Conflicting phylogenetic signals exist between coding and non-coding regions of Laureae plastomes. Our study highlights the importance of evaluating the influence of non-coding regions on tree topology and emphasizes the necessity of examining discordance among different plastid loci in phylogenetic studies.

Introduction

Gene tree discordance is relatively common in phylogenomic studies. The conflicts can be caused by biological factors like incomplete lineage sorting (ILS), hybridization, horizontal gene transfer, gene loss, and gene duplication (*Maddison, 1997; Sun et al., 2015; Gonçalves et al., 2019; Sato et al., 2019*). Most relevant studies have focused on incongruent tree topologies among different genomic compartments (*Sun et al., 2015; Zhao et al., 2016; Walker et al., 2019*) because these genes have evolved independently and their gene tree topologies have been influenced by biological processes. By contrast, relatively few studies have focused on tree conflicts among plastid genes (e.g., *Foster, Henwood & Ho, 2018; Gonçalves et al., 2019; Walker et al., 2019; Zhang et al., 2020*). Usually, plastomes are considered to be uniparentally inherited and to have evolved as a single unit, free from such biological sources of conflict (*Birky, 1995; Wicke et al., 2011*). However, the branched and linear structure of plastid DNA, which arose from recombination-dependent replication, is indicative of recombination (*Oldenburg & Bendich, 2016; Ruhlman et al., 2017*). In addition, biparental inheritance and heteroplasmy (e.g., the presence of different plastomes within an individual or a cell) have been reported in seed plants (*Szmidt, Aldén & Hällgren, 1987; Johnson & Palmer, 1989; Reboud & Zeyl, 1994; Carbonell-Caballero et al., 2015*). Heteroplasmy may, in rare cases, give rise to heteroplasmic recombination, which has been invoked to explain gene tree discordance (*Marshall, Newton & Ritland, 2001; Sullivan et al., 2017; Sancho et al., 2018*). In addition to recombination events, the transfer of genes among plastid, mitochondrial and nuclear genomes; positive selection; tree length (gene evolutionary rate); and GC content may also generate

phylogenomic conflict (e.g., *Stegemann et al., 2003; Smith, 2014; Wysocki et al., 2015; Piot et al., 2018; Saarela et al., 2018; Foster, Henwood & Ho, 2018*). Aside from biological factors, non-biological factors (e.g., outlier genes, uninformative loci, and gaps) may cause conflict as well. For example, *Duvall, Burke & Clark* (*2020*) found that alternative topologies arose from alignment gaps. Given that most studies assume no conflict and treat the plastome as a single unit, taking biological and non-biological factors into consideration and quantifying the extent of conflict among different plastid loci is of great importance (*Wolfe & Randle, 2004*).

Owing to the rapid development of next-generation sequencing (NGS), more plastomes are becoming available at a reasonable cost, driving advances in phylogenomics and promoting a more comprehensive understanding of plant evolution (*Li et al., 2019*). Phylogenetic relationships among Lauraceae (*Song et al., 2017*), as well as many other groups (e.g., *Eserman et al., 2014; Barrett et al., 2016*), have been well resolved using plastome data. In phylogenomic studies of plastomes (*Guo et al., 2017; Gonçalves et al., 2019; Xu et al., 2019; Li et al., 2019*), plastome coding genes have generally been used, and non-coding regions have been excluded. Only a few studies have noted the potential impact of non-coding regions on tree topology. *Parks, Cronn & Liston* (*2009*) revealed that the phylogenetic position of *Pinus albicaulis* Engelm. based on complete plastomes differed from that based on exon sequences. A similar situation also occurred for phylogenetic relationships within Rubiaceae (*Wikström, Bremer & Rydin, 2020*), suggesting that there were conflicting phylogenetic signals between coding- and non-coding regions. Because tree topology is the foundation of comparative studies that infer biogeographic history, phylogenetic diversity and other evolutionary patterns (*Walker et al.,*

2019), the influence of non-coding regions on phylogenetic inference should be evaluated.

Both ILS and hybridization are at play in tree species, which generally have high rates of outcrossing and large population sizes (*Petit & Hampe, 2006; Crowl et al., 2019*). Interspecific hybrids have been described in *Persea* (tribe Perseeae, sister to tribe Cinnamomeae and tribe Laureae), *Cinnamomum* and *Aiouea* (tribe Cinnamomeae) (*van der Werff, 1984; Rohwer et al., 2019*). These processes are perhaps also problematic in Laureae. When combined, such biological processes may make accurate inference of evolutionary relationships in Laureae difficult. Unfortunately, previous phylogenomic studies of Laureae have ignored potential conflicts among different plastid loci and the underlying processes that may have generated them (*Zhao et al., 2018; Song et al., 2019; Tian, Ye & Song, 2019*). These characteristics make Laureae an ideal group in which to explore intra-plastome conflict and its influence on phylogenetic inference.

Tribe Laureae, a species-rich group in the family Lauraceae, is phylogenetically sister to tribe Cinnamomeae (*Song et al., 2019*). It comprises approximately 500 species and 10 genera: *Actinodaphne*, *Adenodaphne*, *Dodecadenia*, *Iteadaphne*, *Laurus*, *Lindera*, *Litsea*, *Neolitsea*, *Parasassafras* and *Sinosassafras* (*van der Werff & Richter, 1996; Chanderbali, van der Werff & Renner, 2001; Li et al., 2004; Li et al., 2008b*). Species of this tribe are evergreen or deciduous and usually occur in the form of trees or shrubs (*Li et al., 2008a*). Their distribution ranges from the Mediterranean region, Asia, and Oceania to North America (*Li et al., 2004*). Some members of Laureae have great ecological and economic value. For example, *Neolitsea sericea* (Bl.) Koidz. is a dominant species found in various evergreen and deciduous broadleaf mixed forests

and in evergreen broadleaf forests (*Wang et al., 2009*), and *Laurus nobilis* L. has been used in remedies for centuries (*Nayak et al., 2006*).

Although Laureae is monophyletic, generic delimitation within this tribe remains unclear (*Kostermans, 1957; Hutchinson, 1964; Li et al., 2008b*). *Adenodaphne*, endemic to New Caledonia, is closely related to *Litsea* (*Chanderbali, van der Werff & Renner, 2001*). However, morphological confusion still exists between this genus and *Litsea*, meaning that their distinctiveness and the monophyly of *Adenodaphne* require further study (*Chanderbali, van der Werff & Renner, 2001*). *Actinodaphne* is polyphyletic and closely related to the monophyletic genus *Neolitsea* (*Li et al., 2007; Li et al., 2008b; Fijridiyanto & Murakami, 2009a*, *2009b*). Although *Fijridiyanto & Murakami* (*2009a*, *2009b*) argued that *Actinodaphne* was monophyletic, the species of *Actinodaphne* sampled in their analyses were totally different from those sampled in *Li et al.* (*2007*) and *Li et al.* (*2008b*). Furthermore, *Lindera* and *Litsea* have been shown to be polyphyletic, with *Dodecadenia*, *Iteadaphne*, *Laurus, Parasassafras* and *Sinosassafras* nested within them (*Li et al., 2004; Li et al., 2008b*). *Liu et al.* (*2017*) used three plastid barcode loci combined with the internal transcribed spacer (ITS) region for species identification and found that the Laureae tree was polytomic. Despite these efforts, phylogenetic relationships among and within these genera have been poorly resolved based on molecular markers like the ITS, the external transcribed spacer (ETS), *matK*, *trnL-F* and *trnH-psbA*. Compared with these molecular markers, complete plastomes have better performance at the species level within Laureae, although generic delimitation still remains unclear due to limited taxon sampling (*Zhao et al., 2018; Song et al., 2019; Tian, Ye & Song, 2019*).

123 Thirty-five plastomes representing 28 species and six genera of Laureae have been published
124 (Table S1). Compared with the vast diversity of Laureae, the published plastome data for this
125 group are relatively limited. Hence, we now report 12 newly sequenced plastomes (Table 1) and
126 combine them with existing plastomes to address three primary goals: (1) reinvestigation of
127 phylogenetic relationships within Laureae; (2) examination of conflict between coding and non-
128 coding regions; and (3) quantification of conflicts among different plastid loci.
129

130 ## Methods

131 **Plant materials, DNA extraction and genome sequencing**

132 Materials from 12 species in five genera (*Actinodaphne obovata* (Nees) Bl., *Iteadaphne caudata*
133 (Nees) H. W. Li, *Lindera erythrocarpa* Makino, *Litsea acutivena* Hay., *L. elongata* (Wall. ex
134 Nees) Benth. et Hook. f., *L. glutinosa* (Lour.) C. B. Rob., *L. dilleniifolia* P. Y. Pai et P. H.
135 Huang, *L. mollis* Hemsl., *L. monopetala* (Roxb.) Pers., *L. pungens* Hemsl., *L. szemaois* (H. Liu)
136 J. Li et H.W. Li, and *Neolitsea pallens* (D. Don) Momiy. et H. Hara) (tribe Laureae, Lauraceae)
137 were collected and identified by the authors (Table 1). Voucher specimens were deposited in the
138 herbarium of the South China Botanical Garden (IBSC) at the Chinese Academy of Sciences. No
139 specific permissions were required for the relevant locations and activities. Including the
140 plastomes downloaded from GenBank and the Lauraceae Chloroplast Genome Database
141 (LCGDB, https://lcgdb.wordpress.com) (Table S1), this study included 47 Laureae plastomes,
142 representing seven genera and all subclades identified by *Song et al.* (*2019*). Twelve plastomes
143 from other tribes were also downloaded (Table S1).

144 Genomic DNA was extracted from silica-gel-dried leaf tissue using the cetyl trimethyl
145 ammonium bromide (CTAB) method (*Doyle & Doyle, 1987*). The yields of genomic DNA
146 extracts were quantified by fluorometric quantification on a Qubit instrument (Invitrogen,
147 Carlsbad, California, USA) using the dsDNA HS kit, and the DNA size distribution was assessed
148 visually on a 1% agarose gel. DNA libraries with an average insert size of 270 bp were prepared
149 by the Beijing Genomics Institute (BGI, Shenzhen, China). Paired-end reads of 2 × 151 bp were
150 generated on the Illumina X ten sequencing system (Illumina Inc.).
151
152 **Plastid genome assembly, annotation and comparison**
153 Low-quality reads and adaptors were removed using Trimmomatric v0.36 (*Bolger, Lohse &*
154 *Usadel, 2014*), generating approximately 3 Gb of high-quality clean reads per sample. The clean
155 reads were analyzed for quality control with FastQC (*Andrews, 2010*) and then used to assemble
156 plastomes with NOVOPlasty v2.7.2 (*Dierckxsens, Mardulyn & Smits, 2016*). To guarantee
157 assembly quality, clean reads were mapped to the assembled plastid genomes using the Burrows-
158 Wheeler Aligner (BWA 0.7.17-r1188 (*Li & Durbin, 2010*)) and samtools 1.9 (*Li et al., 2009*),
159 and were visually checked in Geneious Prime 2019.1.
160 Plastome annotation was performed using the program GeSeq - Annotation of Organellar
161 Genomes (*Tillich et al., 2017*). Start and stop codons were inspected and manually adjusted in
162 Geneious Prime when necessary. Plastomes were submitted to GenBank (MN274947,
163 MN428456–MN428466). Maps of all 12 plastomes were drawn using the
164 OrganellarGenomeDRAW tool (OGDRAW) (*Lohse et al., 2013*). A summary of the newly

sequenced plastomes is presented in Table 2.

To illustrate interspecific sequence variation within Laureae, plastomes of *A. obovata*, *I. caudata*, *Laurus nobilis* (KY085912), *Lindera erythrocarpa*, *Litsea acutivena*, *N. pallens* and *Parasassafras confertiflorum* (Meisn.) D. G. Long (MH729378) were aligned using MAFFT (*Katoh & Standley, 2013*) with default settings. Sequence identity was plotted with the mVISTA program using the LAGAN mode (*Frazer et al., 2004*), with *Lindera glauca* (Siebold et Zucc.) Bl. (MF188124) as a reference.

Phylogenetic reconstruction and tests for selection

To evaluate potential conflicts, phylogenetic trees were constructed using maximum likelihood (ML) methods based on six datasets: (1) complete plastome (cp), (2) coding regions (CDS), (3) non-coding regions (non-CDS), (4) large single copy region (LSC), (5) small single copy region (SSC), and (6) one inverted repeat region (IR).

Sequences were aligned using MAFFT with default settings and manually edited with BioEdit v7.2.5 (*Hall, 1999*) when necessary. The best-fitting DNA substitution models for the six unpartitioned datasets were selected using ModelTest-NG (*Darriba et al., 2020*) under the corrected Akaike Information Critierion (AICc). The aligned sequences and selected DNA substitution models were used for ML analyses, and ML trees were constructed using RAxML-NG (*Kozlov et al., 2019*). We also implemented a partitioning strategy on two datasets, the cp with one IR region removed (cp-reduced) and CDS (configuration details shown in Supplemental File 1). The best partition schemes were inferred with PartitionFinder 2 (*Lanfear et al., 2016*),

and the best partition schemes and models for each partition were used for ML analyses in RAxML-NG.

Because gaps can affect tree topology (*Duvall, Burke & Clark, 2020*), we also performed the following analysis based on the cp dataset. 'Mask Alignment' in Geneious Prime was used to strip the gaps from the MAFFT alignment, with the threshold set to 0 (no gaps), 2%, 10%, 20%, 50% or 75%. The resulting alignments were used to infer ML trees in RAxML-NG.

Positive selection on plastid coding genes has the potential to bias phylogenies (e.g., *Piot et al., 2018; Saarela et al., 2018*), and we therefore performed natural selection tests using CODEML in PAML 4.9j (*Yang, 2007*). Coding genes were extracted and aligned in Geneious Prime using MAFFT, stop codons were removed manually, and the aligned sequences were converted to paml format. To statistically test for positive selection, we compared the performance of two branch models (M0 and M2) for each gene. Three foreground branches were labeled on the unpartitioned CDS ML tree. Likelihood ratio tests (LRT) were performed using pchisq function in R 3.6.2 (*R Core Team, 2018*).

Node support investigation and tree topology tests

Because gene contents were not identical among Cryptocaryeae, *Cassytha*, *Caryodaphnopsis*, *Neocinnamomum* and other clades, the following analyses were performed using a dataset from which six plastomes had been removed (*Beilschmiedia pauciflora* H. W. Li, *Caryodaphnopsis malipoensis* Bing Liu et Y. Yang, *Cassytha filiformis* L., *Cryptocarya chinensis* (Hance) Hemsl. and *Eusideroxylon zwageri* Teijsm. et Binn.).

We extracted all loci (coding regions, introns, tRNA, rRNA and intergenic spacers) using a python script (*Jin, 2019*) and aligned them using MAFFT with default settings. These alignments were used to infer gene trees by rapid bootstrap analyses (option -f a) in RAxML (*Stamatakis, 2014*) with the GTRGAMMA model. The number of bootstrap replicates was set to 1000, as *Simmons & Kessenich* (*2019*) have suggested that fewer replicates may be insufficient to find the optimal gene tree topology. The best-scoring ML trees were used to estimate the species tree with local posterior probability (LPP) (*Sayyari & Mirarab, 2016*) in ASTRAL III (*Zhang et al., 2018*).

We performed constrained maximum likelihood analyses in IQ-TREE (*Nguyen et al., 2014*) to obtain the ML trees that supported different topologies. To understand which loci supported the alternative topologies, we calculated site-wise log-likelihood values for each topology in RAxML using option "-f G". After obtaining site-wise lnL differences, we converted site-wise differences to locus-wise lnL differences (ΔlnL) in R 3.6.2. The lnL differences were plotted against each locus using ggplot2 (*Wickham, 2016*). It has been suggested that loci with an absolute ΔlnL > 2 are statistically significant (*Edwards, 1984*). Therefore, we conducted separate ML analyses on datasets from which these loci (absolute ΔlnL > 2) had been removed to test whether small subsets of sequence matrices determined tree topology (*Shen, Hittinger & Rokas, 2017*).

The Kishino–Hasegawa test (KH test) (*Kishino & Hasegawa, 1989*), Shimodaira-Hasegawa test (SH test) (*Shimodaira & Hasegawa, 1999*) and Approximately-Unbiased test (AU test) (*Shimodaira, 2002*) were used in IQ-TREE to assess the statistical significance of incongruence

based on complete plastomes (including only one copy of the IR regions). We specified 10,000 RELL (resampling of estimated log-likelihoods) replicates for the topological tests.

Results

Plastome features of Laureae

The sizes of the 12 newly generated Laureae plastid genomes ranged from 152,132 bp (*Litsea szemaois*) to 152,916 bp (*Lindera erythrocarpa*) (Table 2), similar to previously published Laureae plastomes (152,211–153,011 bp, Table S1). All had a typical quadripartite structure and were assembled into a single, circular and double-stranded DNA sequence (Fig. 1). The length of the LSC, SSC and IR regions ranged from 93,119 bp (*Litsea szemaois*) to 93,921 bp (*Lindera erythrocarpa*), 18,796 bp (*N. pallens*) to 18,936 bp (*Litsea mollis*), and 20,057 bp (*A. obovata*) to 20,144 bp (*I. caudata*), respectively, with little variation in size (Table 2). The overall GC contents ranged from 39.1% to 39.2%. GC content was unequally distributed within the plastomes; it was highest in IR regions (44.4–44.5%), moderate in LSC regions (37.9–38.1%), and lowest in SSC regions (33.8–34.0%, Table 2).

The 12 newly sequenced plastomes contained 112 single-copy genes: 78 protein-coding genes, 30 tRNA genes, and 4 rRNA genes (Table 2 and Table S2). Sixteen genes had one intron, and two genes had two introns. There were 13 duplicated genes in the IR regions (Table S2), and *rps12*, *ycf1*, and *ycf2* were partly duplicated in the IR regions (Fig. 1).

Phylogenetic reconstruction and positive selection tests

The GTR+I+G4 model was selected for the six unpartitioned datasets (cp, CDS, non-CDS, LSC,

SSC and IR). Perseeae was sister to Cinnamomeae and Laureae (Figs. 2 and S1-S5). All the ML trees indicated the monophyly of Laureae with high bootstrap (BS) support values (99–100%, Figs. 2 and S1-S4), except for the ML tree based on the IR region (71%, Fig. S5). This result was caused by the low variability of the IR region (Fig. S6). In the five ML trees (Figs. 2 and S1-S4), Laureae was divided into three groups. Subclade I included *Lindera communis* Hemsl., *L. glauca* and *L. nacusua* (D. Don) Merr.; subclade II included *Laurus azorica* (Seub.) Franco, *L. nobilis*, *Lindera megaphylla* Hemsl., *Litsea acutivena*, *L. glutinosa*, *L. monopetala* and *L. pungens*; and subclade III included the other Laureae species used in the study. In subclade I, *Lindera glauca* was sister to *L. communis* and *L. nacusua*. In subclade II, *Laurus* was sister to *Litsea acutivena*, *L. glutinosa* and *Lindera megaphylla*, and the position of *Litsea pungens* was unstable (Figs. 2 and S1-S4). *Litsea monopetala* (LAU00063) was embedded within three samples of *Litsea glutinosa* in subclade II, highlighting the necessity of re-identification for *L. monopetala* (LAU00063). Topologies within subclade III based on different datasets were largely congruent (Figs. 2 and S1-S4). In subclade III, samples of *Litsea*, together with *Lindera obtusiloba* Bl., were monophyletic. *Lindera erythrocarpa*, *L. latifolia* Hook. f., *L. metcalfiana* Allen and *L. robusta* (Allen) Tsui were monophyletic as well. *Lindera aggregata*, *L. chunii* Merr., *L. fragrans* Oliv., *L. limprichtii* H. Winkl., *L. pulcherrima* (Wall.) Benth., *L. supracostata* Lec., *L. thomsonii* Allen and *L. thomsonii* var. *vernayana* (Allen) H.P. Tsui formed a well-supported clade. *Neolitsea* was closer to *Actinodaphne* than to other Laureae species.

Subclade II was sister to subclade I based on four unpartitioned datasets (cp, non-CDS, LSC, SSC; Figs. 2 and S2-S4, respectively). However, subclade II was sister to subclade III rather than

subclade I based on the unpartitioned CDS dataset (Fig. S1). Both topologies were strongly supported.

The sister relationship of subclades I and II was confirmed in the ML tree based on partitioned plastomes (one IR removed, cp-reduced dataset; Fig. S7), and subclade II was sister to subclade III in the ML tree based on the partitioned CDS dataset (Fig. S8), indicating that partitioning did not affect our tree topology.

The sister relationship of subclades I and II (BS values ranging from 80% to 92%) was consistently revealed even as the percentage of gaps increased (Table S3), indicating that gaps had no impact on our tree topology.

LRT showed that the dN/dS ratios of labeled lineages (subclades I, II and III) were not significantly different from background ($p > 0.05$), of which dN/dS ratios were less than one (Table S4), suggesting that there was no positive selection on the plastid genes.

Investigating incongruent nodes and differences in tree topology

The tree topology inferred from ASTRAL III (Fig. 3) was largely congruent with that of the ML trees (Figs. 2 and S1–S4), except that the former showed a sister relationship of subclade I and subclade III. We performed constrained maximum likelihood analyses in IQ-TREE and obtained three suboptimal ML trees that supported the subclade II–subclade I (called T1 hereafter), subclade II–subclade III (T2) and subclade I–subclade III (T3) affinities. We extracted 243 loci and assessed how each locus supported one of the three topologies by examining the gene-wise log-likelihoods (Fig. 4). T1 was strongly supported by six loci (*rpoC1* intron, *trnG-trnfM*, *ndhA*

292 intron, *psaJ-rpl33*, *rpl2-rpl23* and *petN-psbM*; absolute ΔlnL > 2); T2 was strongly supported by
293 three loci (*psaB*, *trnS-ycf3* and *ycf2*; absolute ΔlnL > 2); and T3 was moderately supported by
294 one locus (*clpP* intron1; absolute ΔlnL > 1 and < 2) (Table S5). The sum of absolute ΔlnL of T1
295 was higher than that of T2 and T3 (Fig. 4), suggesting that our data support the topology of T1
296 rather than T2 or T3. After the removal of six loci (*rpoC1* intron, *trnG-trnfM*, *ndhA* intron, *psaJ-*
297 *rpl33*, *rpl2-rpl23* and *petN-psbM*), a sister relationship of subclade II and subclade III was
298 revealed (Fig. S9). After the removal of three loci (*psaB*, *trnS-ycf3*, and *ycf2*), subclade II was
299 sister to subclade I (Fig. S10). These results underscore the decisive role played by small subsets
300 of loci in phylogenetic inference.

301 The topological tests showed that T2 did not differ significantly from T1 ($p > 0.05$, Table S6).
302 T3 was statistically rejected by the KH and AU tests ($p < 0.05$) but not by the Shimodaira-
303 Hasegawa (SH) test ($p = 0.0505$). That T3 was rejected according to the KH and AU tests
304 suggests that the sister relationship between subclades I and III may be misleading.
305

306 ## Discussion

307 ### Plastome features

308 It has been noted that most plastid genomes of land plants and algae range from 120 to 160
309 kilobase pairs (kb) in length (*Palmer, 1985*). In this study, the plastid genome sizes of 12 species
310 from five Laureae genera ranged from 152,132 bp to 152,916 bp, indicating that plastid genome
311 size was conserved within Laureae. GC content was highest in the IR region rather than in the
312 single copy regions, owing to the presence of a ribosomal RNA gene cluster in the IR region,

313 consistent with a previous study (*Huotari & Korpelainen, 2012*). GC contents of the IR, LSC and
314 SSC regions of the newly sequenced plastomes were identical to those of nine *Lindera* species
315 studied earlier (*Zhao et al., 2018*). In contrast to the gene losses recognized in several Lauraceae
316 lineages (*Song et al., 2017*), our analysis revealed that gene content among Laureae was highly
317 conserved. *Song et al.* (*2017*) suggested that plastome contraction in Lauraceae was largely
318 driven by fragment loss events in the IR regions. In our study, we found no gene loss among
319 Laureae plastomes.
320
321 **Phylogenetic relationships within Laureae**
322 Previous phylogenetic studies (*Song et al., 2017; Zhao et al., 2018*) based on complete plastomes
323 suggested that Laureae was sister to Cinnamomeae and that together they were sister to Perseeae.
324 The same phylogenetic relationships among these groups were recognized in our study (Figs. 2
325 and 3). In previous work, *Actinodaphne* and *Neolitsea* were resolved as monophyletic groups
326 based on *matK*, ITS and rpb2 (*Fijridiyanto & Murakami, 2009a*, *2009b*), but *Actinodaphne* was
327 not a monophyletic group based on complete plastid genomes (*Song et al., 2019*). In this study,
328 the non-monophyletic status of *Actinodaphne* was supported. The conclusion of *Actinodaphne*
329 monophyly may have been caused by sampling bias in previous studies (*Fijridiyanto &*
330 *Murakami, 2009b*, *2009a*). The monophyly of *Neolitsea* can be neither rejected nor supported in
331 the present study. *Actinodaphne cupularis* (Hemsl.) Gamble was grouped with *Neolitsea*
332 *oblongifolia* Merr. et Chun, *N. pallens* and *N. chui* Merr. with low bootstrap support (54%; Fig.
333 2), and sampling of *Neolitsea* and related genera was limited. *Lindera* and *Litsea* were

polyphyletic in our analysis, consistent with previous studies (*Li et al., 2008b; Fijridiyanto & Murakami, 2009b*). The phylogenetic position of *P. confertiflorum* was unresolved based on ETS and ITS (*Li et al., 2008b*), and the ambiguity of its position still remains, despite the integration of complete plastid genomes in our analysis and a previous study (*Liao, Ye & Song, 2018*).

Subclade III was sister to subclade I and II in our study, consistent with previous analyses (*Zhao et al., 2018; Song et al., 2019; Tian, Ye & Song, 2019*). The three *Lindera* species in subclade I share common morphological traits, such as alternate and pinninerved leaves, a persistent involucre, vegetative terminal buds in inflorescences and 3-merous flowers (*Li et al., 2008a*). However, these characters also occur in several members of the other two subclades (e.g., *Lindera benzoin* (L.) Bl. and *Laurus nobilis*), perhaps resulting from convergent and/or parallel evolution (*Li et al., 2008b*). These traits are not good indicators for delimiting the three subclades of Laureae. In subclade III, the trinerved or triplinerved species of *Lindera* (*Lindera aggregata*, *L. chunii*, *L. fragrans*, *L. limprichtii*, *L. pulcherrima*, *L. supracostata*, *L. thomsonii* and *L. thomsonii* var. *vernayana*) formed a well-supported clade in both our study and that of *Tian, Ye & Song* (*2019*). However, triplinerved leaves also exist in most species of *Neolitsea* (*Li et al., 2008b; Li et al., 2008a*). Therefore, traditional morphological traits are of limited use in taxon delimitation, even within subclades of Laureae. Given the limited samples and data in our analyses, more sampling and DNA sequences are needed to further elucidate the relationships within Laureae.

Phylogenetic incongruence in the plastome

Although many studies have treated plastid protein-coding genes or the complete plastome as a single unit (e.g., *Song et al., 2019; Tian, Ye & Song, 2019*), potential conflicts among sequence types (i.e., coding vs. non-coding regions) have been reported in several studies. By comparing phylogenies based on complete plastomes and coding regions (*Yu et al., 2017*), it was inferred that non-coding regions did not significantly influence the tree topology of Theaceae. By contrast, non-coding regions had an impact on the phylogenetic relationships of several tribes in Rubiaceae (*Wikström, Bremer & Rydin, 2020*) and subtribes in Poaceae (*Saarela et al., 2018*). A conflicting signal between coding and non-coding regions was also reported in Leguminosae (*Zhang et al., 2020*). In this study, inclusion of non-coding regions altered tree topology in the tribe Laureae, suggesting the existence of a conflicting signal between coding and non-coding regions. Non-coding regions are often discarded for being uninformative, or for being misleading due to saturation at deep time scales (*Foster, Henwood & Ho, 2018*). In our study, tree topologies based on coding and non-coding regions were largely congruent, except for the relationships among the three subclades (Figs. S1–S2), indicating that non-coding regions are as informative as coding regions in Laureae. Thus, it is imperative to evaluate the influence of non-coding regions on tree topology rather than treating the whole plastome as a single unit or simply excluding non-coding regions from phylogenetic analysis.

To accommodate the conflicts among different plastid regions, a species tree was inferred through summary coalescent analysis. It has been suggested that the coalescent method is more robust than the concatenation method when the level of ILS is high (*Liu, Xi & Davis, 2014; Mirarab, Bayzid & Warnow, 2014*). High ILS tends to occur when the time interval between

consecutive speciation events is short (*Sun et al., 2015; Sato et al., 2019*), and the core Lauraceae group (Perseeae, Cinnamomeae and Laureae) is thought to have undergone a rapid radiation (*Chanderbali, van der Werff & Renner, 2001; Rohwer & Rudolph, 2005; Nie, Wen & Sun, 2007*). We therefore chose to implement the coalescent method. Nonetheless, it should be noted that, with this method, short and uninformative loci may lead to problematic gene trees and therefore result in a less accurate species tree (*Xi, Liu & Davis, 2015; Springer & Gatesy, 2016*). In our study, only nine of 243 loci (*rpoC1* intron, *trnG-trnfM*, *ndhA* intron, *psaJ-rpl33*, *rpl2-rpl23*, *petN-psbM*, *psaB*, *trnS-ycf3*, and *ycf2*) had a strong phylogenetic signal at the contentious node. The other 234 loci with weak phylogenetic signals may have resulted in gene trees with uncertainties and led to inaccurate topology at this node.

Exploration of the factors that underlie conflicts in phylogenetic signals is of great importance—but it is also challenging. Previous studies have examined whether biological and non-biological factors contribute to such conflicts (e.g., *Duvall, Burke & Clark, 2020; Zhang et al., 2020*). For example, gaps have been found to cause alternate, but conflicting topologies in Poaceae (*Duvall, Burke & Clark, 2020*). However, the inclusion of alignment gaps did not alter our tree topology (Table S3). Although previous studies indicated that partitioning improves phylogenetic inference (*Xi et al., 2012*), ML tree topologies based on partitioned and unpartitioned datasets did not differ significantly in our study. It has been suggested that plastid genes under positive selection may bias phylogenies (e.g., *Piot et al., 2018; Saarela et al., 2018*). Although *psaB* and *ycf2* were shown to influence topology, neither gene evolved under positive selection, suggesting that natural selection is not the cause of the conflict. In this study, the low

support values and short branch lengths of the estimated species tree (Fig. 3) suggested that each locus had a significantly incongruent topology and may indicate the existence of ILS. High levels of ILS are thought to yield similar numbers of loci supporting alternative topologies (*Huson et al., 2005*). In our study, the numbers of loci supporting each topology were different (six for T1, three for T2, and zero for T3 after exclusion of loci with absolute $\Delta \ln L \leq 2$), suggesting that ILS may not be the primary cause of the discordance among loci. Another plausible explanation for the conflict is heteroplasmic recombination, which can occur in species with biparental plastome inheritance (*Walker et al., 2019*). Although heteroplasmic recombination has been reported with clear evidence in *Brachypodium* and *Picea* (*Sullivan et al., 2017; Sancho et al., 2018*), to our knowledge it has never been documented in Lauraceae. Based on the data reported here, it is too early to draw a firm conclusion about the causes of the conflict in phylogenetic signals. Although fully resolved phylogenies may still remain elusive based on different genomic compartments (i.e., nuclear, mitochondrial and plastid), phylogenomic studies that incorporate these compartments can provide new insights into tree discordance and its underlying causes (*Koenen et al., 2020*). Therefore, more genetic information (e.g., nuclear genes) will be required to solve this problem in future work.

Conclusion

In summary, this study revealed that Laureae plastomes are conserved in structure, size and gene content. A conflicting phylogenetic signal was detected between coding and non-coding regions, suggesting that the plastid genome should not be treated as a single unit. ML trees based on

418 coding and non-coding regions were largely congruent except at the contentious node, indicating
419 that coding regions are as informative as non-coding regions and that the influence of non-coding
420 regions on tree inference should be evaluated. We also found that small subsets of plastome loci
421 determined the topology at specific nodes, consistent with the results of a previous study (*Shen,*
422 *Hittinger & Rokas, 2017*). Through quantification and analysis of intra-plastome conflicts, the
423 sister relationship of subclade I (including *Lindera communis*, *L. glauca* and *L. nacusua*) and II
424 (including *Laurus azorica*, *L. nobilis*, *Lindera megaphylla*, *Litsea acutivena*, *L. glutinosa*, *L.*
425 *monopetala* and *L. pungens*) was supported by our study. Biological factors may contribute to
426 the conflicts among plastid loci; however, more information is needed to determine the
427 underlying mechanism(s).
428
429 **Acknowledgements**
430 The authors thank Yu-Ying Zhou and Chen-Xin Ma for assistance with the DNA experiments. They also thank
431 Feng Song for her kind help in plastid genome assembly and annotation. The authors would like to thank TopEdit
432 (www.topeditsci.com) for English language editing of this manuscript.
433
434
435
436 **Reference**
437 Andrews S. 2010. FastQC: a quality control tool for high throughput sequence data. *Available at*
438 *http://www.bioinformatics.babraham.ac.uk/projects/fastqc*
439 Barrett CF, Baker WJ, Comer JR, Conran JG, Lahmeyer SC, Leebens-Mack JH, Li J, Lim GS, Mayfield-Jones DR,
440 Perez L, Medina J, Pires JC, Santos C, Wm. Stevenson D, Zomlefer WB, Davis JI. 2016. Plastid genomes
441 reveal support for deep phylogenetic relationships and extensive rate variation among palms and other
442 commelinid monocots. *New Phytologist* 209:855-870 DOI: 10.1111/nph.13617.
443 Birky CW. 1995. Uniparental inheritance of mitochondrial and chloroplast genes: mechanisms and evolution.
444 *Proceedings of the National Academy of Sciences of the United States of America* 92:11331-11338 DOI:

10.1073/pnas.92.25.11331.
Bolger AM, Lohse M, Usadel B. 2014. Trimmomatic: a flexible trimmer for Illumina sequence data. *Bioinformatics* 30:2114-2120 DOI: 10.1093/bioinformatics/btu170.
Carbonell-Caballero J, Alonso R, Ibañez V, Terol J, Talon M, Dopazo J. 2015. A phylogenetic analysis of 34 chloroplast genomes elucidates the relationships between wild and domestic species within the genus *Citrus*. *Molecular Biology and Evolution* 32:2015-2035 DOI: 10.1093/molbev/msv082.
Chanderbali AS, van der Werff H, Renner SS. 2001. Phylogeny and historical biogeography of Lauraceae: Evidence from the chloroplast and nuclear genomes. *Annals of the Missouri Botanical Garden* 88:104-134 DOI: 10.2307/2666133.
Crowl AA, Manos PS, McVay JD, Lemmon AR, Lemmon EM, Hipp AL. 2019. Uncovering the genomic signature of ancient introgression between white oak lineages (*Quercus*). *New Phytologist* DOI: 10.1111/nph.15842.
Darriba D, Posada D, Kozlov AM, Stamatakis A, Morel B, Flouri T, Crandall K. 2020. ModelTest-NG: A new and scalable tool for the selection of DNA and protein evolutionary models. *Molecular Biology and Evolution* 37:291-294 DOI: 10.1093/molbev/msz189.
Dierckxsens N, Mardulyn P, Smits G. 2016. NOVOPlasty: de novo assembly of organelle genomes from whole genome data. *Nucleic Acids Research* 45:e18-e18 DOI: 10.1093/nar/gkw955.
Doyle JJ, Doyle JL. 1987. A rapid DNA isolation procedure for small quantities of fresh leaf tissue. *Phytochemical Bulletin* 19:11-15.
Duvall MR, Burke SV, Clark DC. 2020. Plastome phylogenomics of Poaceae: alternate topologies depend on alignment gaps. *Botanical Journal of the Linnean Society* 192:9-20 DOI: 10.1093/botlinnean/boz060.
Edwards AWF. 1984. *Likelihood*. Cambridge: Cambridge University Press.
Eserman LA, Tiley GP, Jarret RL, Leebens-Mack JH, Miller RE. 2014. Phylogenetics and diversification of morning glories (tribe Ipomoeeae, Convolvulaceae) based on whole plastome sequences. *American Journal of Botany* 101:92-103 DOI: 10.3732/ajb.1300207.
Fijridiyanto IA, Murakami N. 2009a. Molecular systematics of Malesian *Litsea* Lam. and putative related genera (Lauraceae). *Acta Phytotaxonomica et Geobotanica* 60:1-18 DOI: 10.18942/apg.KJ00005576218.
Fijridiyanto IA, Murakami N. 2009b. Phylogeny of *Litsea* and related genera (Laureae-Lauraceae) based on analysis of rpb2 gene sequences. *Journal of Plant Research* 122:283-298 DOI: 10.1007/s10265-009-0218-8.
Foster CSP, Henwood MJ, Ho SYW. 2018. Plastome sequences and exploration of tree-space help to resolve the phylogeny of riceflowers (Thymelaeaceae: *Pimelea*). *Molecular Phylogenetics and Evolution* 127:156-167 DOI: 10.1016/j.ympev.2018.05.018.
Frazer KA, Pachter L, Poliakov A, Rubin EM, Dubchak I. 2004. VISTA: computational tools for comparative genomics. *Nucleic Acids Research* 32:W273-W279 DOI: 10.1093/nar/gkh458.
Gonçalves DJP, Simpson BB, Ortiz EM, Shimizu GH, Jansen RK. 2019. Incongruence between gene trees and species trees and phylogenetic signal variation in plastid genes. *Molecular Phylogenetics and Evolution* 138:219-232 DOI: 10.1016/j.ympev.2019.05.022.
Guo X, Liu J, Hao G, Zhang L, Mao K, Wang X, Zhang D, Ma T, Hu Q, Al-Shehbaz IA, Koch MA. 2017. Plastome phylogeny and early diversification of Brassicaceae. *BMC Genomics* 18:176 DOI: 10.1186/s12864-017-3555-3.
Hall TA. 1999. BioEdit: a user-friendly biological sequence alignment editor and analysis program for Windows 95/98/NT. *Nucleic Acids Symposium Series* 41:95-98.

Huotari T, Korpelainen H. 2012. Complete chloroplast genome sequence of *Elodea canadensis* and comparative analyses with other monocot plastid genomes. *Gene* 508:96-105 DOI: 10.1016/j.gene.2012.07.020.

Huson DH, Klöpper T, Lockhart PJ, Steel MA. 2005. Reconstruction of reticulate networks from gene trees. In: Miyano S, Mesirov J, Kasif S, Istrail S, Pevzner PA, Waterman M, eds. *Research in Computational Molecular Biology*. Berlin: Springer, 233-249.

Hutchinson J. 1964. *The Genera of Flowering Plants (Docotyledonae)*. Oxford: Clarendon Press.

Jin J-J. 2019. PersonalUtilities. *Available at https://github.com/Kinggerm/PersonalUtilities* (accessed 15 Oct 2019).

Johnson LB, Palmer JD. 1989. Heteroplasmy of chloroplast DNA in *Medicago*. *Plant Molecular Biology* 12:3-11 DOI: 10.1007/BF00017442.

Katoh K, Standley DM. 2013. MAFFT multiple sequence alignment software version 7: improvements in performance and usability. *Molecular Biology and Evolution* 30:772-780 DOI: 10.1093/molbev/mst010.

Kishino H, Hasegawa M. 1989. Evaluation of the maximum likelihood estimate of the evolutionary tree topologies from DNA sequence data, and the branching order in hominoidea. *Journal of Molecular Evolution* 29:170-179 DOI: 10.1007/bf02100115.

Koenen EJM, Ojeda DI, Steeves R, Migliore J, Bakker FT, Wieringa JJ, Kidner C, Hardy OJ, Pennington RT, Bruneau A, Hughes CE. 2020. Large-scale genomic sequence data resolve the deepest divergences in the legume phylogeny and support a near-simultaneous evolutionary origin of all six subfamilies. *New Phytologist* 225:1355-1369 DOI: 10.1111/nph.16290.

Kostermans AJGH. 1957. Lauraceae. *Reinwardtia* 4:193-256.

Kozlov AM, Darriba D, Flouri T, Morel B, Stamatakis A. 2019. RAxML-NG: a fast, scalable and user-friendly tool for maximum likelihood phylogenetic inference. *Bioinformatics* 35:4453-4455 DOI: 10.1093/bioinformatics/btz305.

Lanfear R, Frandsen PB, Wright AM, Senfeld T, Calcott B. 2016. PartitionFinder 2: New methods for selecting partitioned models of evolution for molecular and morphological phylogenetic analyses. *Molecular Biology and Evolution* 34:772-773 DOI: 10.1093/molbev/msw260.

Li H-T, Yi T-S, Gao L-M, Ma P-F, Zhang T, Yang J-B, Gitzendanner MA, Fritsch PW, Cai J, Luo Y, Wang H, van der Bank M, Zhang S-D, Wang Q-F, Wang J, Zhang Z-R, Fu C-N, Yang J, Hollingsworth PM, Chase MW, Soltis DE, Soltis PS, Li D-Z. 2019. Origin of angiosperms and the puzzle of the Jurassic gap. *Nature Plants* 5:461-470 DOI: 10.1038/s41477-019-0421-0.

Li H-W, Li J, Huang P-H, Wei F-N, Tsui H-P, van der Werff H. 2008a. Lauraceae. In: Wu Z-Y, Raven PH, Hong D-Y, eds. *Flora of China*. Beijing & Saint Louis: Science Press & Missouri Botanical Garden.

Li H, Durbin R. 2010. Fast and accurate long-read alignment with Burrows–Wheeler transform. *Bioinformatics* 26:589-595 DOI: 10.1093/bioinformatics/btp698.

Li H, Handsaker B, Wysoker A, Fennell T, Ruan J, Homer N, Marth G, Abecasis G, Durbin R, Subgroup GPDP. 2009. The Sequence Alignment/Map format and SAMtools. *Bioinformatics* 25:2078-2079 DOI: 10.1093/bioinformatics/btp352.

Li J, Christophel DC, Conran JG, Li H-W. 2004. Phylogenetic relationships within the 'core' Laureae (*Litsea* complex, Lauraceae) inferred from sequences of the chloroplast gene matK and nuclear ribosomal DNA ITS regions. *Plant Systematics and Evolution* 246:19-34 DOI: 10.1007/s00606-003-0113-z.

Li J, Conran JG, Christophel DC, Li Z-M, Li L, Li H-W. 2008b. Phylogenetic relationships of the *Litsea* complex and core Laureae (Lauraceae) using ITS and ETS sequences and morphology. *Annals of the Missouri*

Botanical Garden 95:580-600 DOI: 10.3417/2006125.9504.

Li L, Li J, Conran JG, Li H-W. 2007. Phylogeny of *Neolitsea* (Lauraceae) inferred from Bayesian analysis of nrDNA ITS and ETS sequences. *Plant Systematics and Evolution* 269:203-221 DOI: 10.1007/s00606-007-0580-8.

Liao Q, Ye T, Song Y. 2018. Complete chloroplast genome sequence of a subtropical tree, *Parasassafras confertiflorum* (Lauranceae). *Mitochondrial DNA Part B* 3:1216-1217 DOI: 10.1080/23802359.2018.1532331.

Liu L, Xi Z, Davis CC. 2014. Coalescent methods are robust to the simultaneous effects of long branches and incomplete lineage sorting. *Molecular Biology and Evolution* 32:791-805 DOI: 10.1093/molbev/msu331.

Liu Z-F, Ci X-Q, Li L, Li H-W, Conran JG, Li J. 2017. DNA barcoding evaluation and implications for phylogenetic relationships in Lauraceae from China. *PLOS ONE* 12:e0175788 DOI: 10.1371/journal.pone.0175788.

Lohse M, Drechsel O, Kahlau S, Bock R. 2013. OrganellarGenomeDRAW—a suite of tools for generating physical maps of plastid and mitochondrial genomes and visualizing expression data sets. *Nucleic Acids Research* 41:W575-W581.

Maddison WP. 1997. Gene Trees in Species Trees. *Systematic Biology* 46:523-536 DOI: 10.1093/sysbio/46.3.523.

Marshall HD, Newton C, Ritland K. 2001. Sequence-repeat polymorphisms exhibit the signature of recombination in Lodgepole pine chloroplast DNA. *Molecular Biology and Evolution* 18:2136-2138 DOI: 10.1093/oxfordjournals.molbev.a003757.

Mirarab S, Bayzid MS, Warnow T. 2014. Evaluating summary methods for multilocus species tree estimation in the presence of incomplete lineage sorting. *Systematic Biology* 65:366-380 DOI: 10.1093/sysbio/syu063.

Nayak S, Nalabothu P, Sandiford S, Bhogadi V, Adogwa A. 2006. Evaluation of wound healing activity of *Allamanda cathartica* L. and *Laurus nobilis* L. extracts on rats. *BMC Complementary and Alternative Medicine* 6:12 DOI: 10.1186/1472-6882-6-12.

Nguyen L-T, Schmidt HA, von Haeseler A, Minh BQ. 2014. IQ-TREE: a fast and effective stochastic algorithm for estimating maximum-likelihood phylogenies. *Molecular Biology and Evolution* 32:268-274 DOI: 10.1093/molbev/msu300.

Nie Z-L, Wen J, Sun H. 2007. Phylogeny and biogeography of *Sassafras* (Lauraceae) disjunct between eastern Asia and eastern North America. *Plant Systematics and Evolution* 267:191-203 DOI: 10.1007/s00606-007-0550-1.

Oldenburg DJ, Bendich AJ. 2016. The linear plastid chromosomes of maize: terminal sequences, structures, and implications for DNA replication. *Current Genetics* 62:431-442 DOI: 10.1007/s00294-015-0548-0.

Palmer JD. 1985. Comparative organization of chloroplast genomes. *Annual Review of Genetics* 19:325-354 DOI: 10.1146/annurev.ge.19.120185.001545.

Parks M, Cronn R, Liston A. 2009. Increasing phylogenetic resolution at low taxonomic levels using massively parallel sequencing of chloroplast genomes. *BMC Biology* 7:84 DOI: 10.1186/1741-7007-7-84.

Petit RJ, Hampe A. 2006. Some evolutionary consequences of being a tree. *Annual Review of Ecology, Evolution, and Systematics* 37:187-214 DOI: 10.1146/annurev.ecolsys.37.091305.110215.

Piot A, Hackel J, Christin P-A, Besnard G. 2018. One-third of the plastid genes evolved under positive selection in PACMAD grasses. *Planta* 247:255-266 DOI: 10.1007/s00425-017-2781-x.

R Core Team. 2018. R: A language and environment for statistical computing. *Available at* http://www.R-

project.org/ (accessed 12 Dec 2019).
Reboud X, Zeyl C. 1994. Organelle inheritance in plants. *Heredity* 72:132-140 DOI: 10.1038/hdy.1994.19.
Rohwer JG, Rudolph B. 2005. Jumping genera: the phylogenetic positions of *Cassytha*, *Hypodaphnis*, and *Neocinnamomum* (Lauraceae) based on different analyses of *trnK* intron sequences. *Annals of the Missouri Botanical Garden* 1:153-178.
Rohwer JG, Trofimov D, Mayland-Quellhorst E, Albach D. 2019. Incongruence of morphological determinations and DNA barcode sequences: a case study in *Cinnamomum* (Lauraceae). *Willdenowia* 49:383-400 DOI: 10.3372/wi.49.49309.
Ruhlman TA, Zhang J, Blazier JC, Sabir JSM, Jansen RK. 2017. Recombination-dependent replication and gene conversion homogenize repeat sequences and diversify plastid genome structure. *American Journal of Botany* 104:559-572 DOI: 10.3732/ajb.1600453.
Saarela JM, Burke SV, Wysocki WP, Barrett MD, Clark LG, Craine JM, Peterson PM, Soreng RJ, Vorontsova MS, Duvall MR. 2018. A 250 plastome phylogeny of the grass family (Poaceae): topological support under different data partitions. *PeerJ* 6:e4299 DOI: 10.7717/peerj.4299.
Sancho R, Cantalapiedra CP, López-Alvarez D, Gordon SP, Vogel JP, Catalán P, Contreras-Moreira B. 2018. Comparative plastome genomics and phylogenomics of *Brachypodium*: flowering time signatures, introgression and recombination in recently diverged ecotypes. *New Phytologist* 218:1631-1644 DOI: 10.1111/nph.14926.
Sato JJ, Bradford TM, Armstrong KN, Donnellan SC, Echenique-Diaz LM, Begué-Quiala G, Gámez-Díez J, Yamaguchi N, Truong Nguyen S, Kita M, Ohdachi SD. 2019. Post K-Pg diversification of the mammalian order Eulipotyphla as suggested by phylogenomic analyses of ultra-conserved elements. *Molecular Phylogenetics and Evolution* 141:106605 DOI: 10.1016/j.ympev.2019.106605.
Sayyari E, Mirarab S. 2016. Fast coalescent-based computation of local branch support from quartet frequencies. *Molecular Biology and Evolution* 33:1654-1668 DOI: 10.1093/molbev/msw079.
Shen X-X, Hittinger CT, Rokas A. 2017. Contentious relationships in phylogenomic studies can be driven by a handful of genes. *Nature Ecology & Evolution* 1:0126 DOI: 10.1038/s41559-017-0126.
Shimodaira H. 2002. An approximately unbiased test of phylogenetic tree selection. *Systematic Biology* 51:492-508 DOI: 10.1080/10635150290069913.
Shimodaira H, Hasegawa M. 1999. Multiple comparisons of log-likelihoods with applications to phylogenetic inference. *Molecular Biology and Evolution* 16:1114-1114.
Simmons MP, Kessenich J. 2019. Divergence and support among slightly suboptimal likelihood gene trees. *Cladistics* DOI: 10.1111/cla.12404.
Smith DR. 2014. Mitochondrion-to-plastid DNA transfer: it happens. *New Phytologist* 202:736-738 DOI: 10.1111/nph.12704.
Song Y, Yu W-B, Tan Y, Jin J, Wang B, Yang J-B, Liu B, Corlett RT. 2019. Plastid phylogenomics improve phylogenetic resolution in the Lauraceae. *Journal of Systematics and Evolution* DOI: 10.1111/jse.12536.
Song Y, Yu WB, Tan Y, Liu B, Yao X, Jin J, Padmanaba M, Yang JB, Corlett RT. 2017. Evolutionary comparisons of the chloroplast genome in Lauraceae and insights into loss events in the Magnoliids. *Genome Biology and Evolution* 9:2354-2364 DOI: 10.1093/gbe/evx180.
Springer MS, Gatesy J. 2016. The gene tree delusion. *Molecular Phylogenetics and Evolution* 94:1-33 DOI: 10.1016/j.ympev.2015.07.018.

Stamatakis A. 2014. RAxML version 8: a tool for phylogenetic analysis and post-analysis of large phylogenies. *Bioinformatics* 30:1312-1313 DOI: 10.1093/bioinformatics/btu033.

Stegemann S, Hartmann S, Ruf S, Bock R. 2003. High-frequency gene transfer from the chloroplast genome to the nucleus. *Proceedings of the National Academy of Sciences of the United States of America* 100:8828 DOI: 10.1073/pnas.1430924100.

Sullivan AR, Schiffthaler B, Thompson SL, Street NR, Wang X-R. 2017. Interspecific plastome recombination reflects ancient reticulate evolution in *Picea* (Pinaceae). *Molecular Biology and Evolution* 34:1689-1701 DOI: 10.1093/molbev/msx111.

Sun M, Soltis DE, Soltis PS, Zhu X, Burleigh JG, Chen Z. 2015. Deep phylogenetic incongruence in the angiosperm clade Rosidae. *Molecular Phylogenetics and Evolution* 83:156-166 DOI: 10.1016/j.ympev.2014.11.003.

Szmidt AE, Aldén T, Hällgren J-E. 1987. Paternal inheritance of chloroplast DNA in *Larix*. *Plant Molecular Biology* 9:59-64 DOI: 10.1007/BF00017987.

Tian X, Ye J, Song Y. 2019. Plastome sequences help to improve the systematic position of trinerved *Lindera* species in the family Lauraceae. *PeerJ* 7:e7662 DOI: 10.7717/peerj.7662.

Tillich M, Lehwark P, Pellizzer T, Ulbricht-Jones ES, Fischer A, Bock R, Greiner S. 2017. GeSeq - versatile and accurate annotation of organelle genomes. *Nucleic Acids Research* 45:W6-W11 DOI: 10.1093/nar/gkx391.

van der Werff H. 1984. Notes on neotropical Lauraceae. *Annals of the Missouri Botanical Garden* 71:1180-1183 DOI: 10.2307/2399252.

van der Werff H, Richter HG. 1996. Toward an improved classification of Lauraceae. *Annals of the Missouri Botanical Garden* 83:409-418 DOI: 10.2307/2399870.

Walker JF, Walker-Hale N, Vargas OM, Larson DA, Stull GW. 2019. Characterizing gene tree conflict in plastome-inferred phylogenies. *PeerJ* 7:e7747 DOI: 10.7717/peerj.7747.

Wang G, Zhao C, Chen Y, Cheng C, Zhao Y. 2009. National key protected plant flora and distribution characteristic in Zhoushan Islands. *Journal of Zhejiang Forestry Science and Technology* 29:43-47.

Wicke S, Schneeweiss GM, dePamphilis CW, Müller KF, Quandt D. 2011. The evolution of the plastid chromosome in land plants: gene content, gene order, gene function. *Plant Molecular Biology* 76:273-297 DOI: 10.1007/s11103-011-9762-4.

Wickham H. 2016. *ggplot2: elegant graphics for data analysis*. New York: Springer-Verlag.

Wikström N, Bremer B, Rydin C. 2020. Conflicting phylogenetic signals in genomic data of the coffee family (Rubiaceae). *Journal of Systematics and Evolution* DOI: 10.1111/jse.12566.

Wolfe AD, Randle CP. 2004. Recombination, heteroplasmy, haplotype polymorphism, and paralogy in plastid genes: implications for plant molecular systematics. *Systematic Botany* 29:1011-1020.

Wysocki WP, Clark LG, Attigala L, Ruiz-Sanchez E, Duvall MR. 2015. Evolution of the bamboos (Bambusoideae; Poaceae): a full plastome phylogenomic analysis. *BMC Evolutionary Biology* 15:50 DOI: 10.1186/s12862-015-0321-5.

Xi Z, Liu L, Davis CC. 2015. Genes with minimal phylogenetic information are problematic for coalescent analyses when gene tree estimation is biased. *Molecular Phylogenetics and Evolution* 92:63-71 DOI: 10.1016/j.ympev.2015.06.009.

Xi Z, Ruhfel BR, Schaefer H, Amorim AM, Sugumaran M, Wurdack KJ, Endress PK, Matthews ML, Stevens PF, Mathews S, Davis CC. 2012. Phylogenomics and a posteriori data partitioning resolve the Cretaceous angiosperm radiation Malpighiales. *Proceedings of the National Academy of Sciences of the United States*

650 *of America* 109:17519-17524 DOI: 10.1073/pnas.1205818109.
651 Xu W-Q, Losh J, Chen C, Li P, Wang R-H, Zhao Y-P, Qiu Y-X, Fu C-X. 2019. Comparative genomics of figworts
652 (Scrophularia, Scrophulariaceae), with implications for the evolution of Scrophularia and Lamiales.
653 *Journal of Systematics and Evolution* 57:55-65 DOI: 10.1111/jse.12421.
654 Yang Z. 2007. PAML 4: Phylogenetic Analysis by Maximum Likelihood. *Molecular Biology and Evolution*
655 24:1586-1591 DOI: 10.1093/molbev/msm088.
656 Yu XQ, Gao LM, Soltis DE, Soltis PS, Yang JB, Fang L, Yang SX, Li DZ. 2017. Insights into the historical
657 assembly of East Asian subtropical evergreen broadleaved forests revealed by the temporal history of the
658 tea family. *New Phytologist* 215:1235-1248 DOI: doi:10.1111/nph.14683.
659 Zhang C, Rabiee M, Sayyari E, Mirarab S. 2018. ASTRAL-III: polynomial time species tree reconstruction from
660 partially resolved gene trees. *BMC Bioinformatics* 19:153 DOI: 10.1186/s12859-018-2129-y.
661 Zhang R, Wang Y-H, Jin J-J, Stull GW, Bruneau A, Cardoso D, de Queiroz LP, Moore MJ, Zhang S-D, Chen S-Y,
662 Wang J, Li D-Z, Yi T-S. 2020. Exploration of plastid phylogenomic conflict yields new insights into the
663 deep relationships of Leguminosae. *Systematic Biology* DOI: 10.1093/sysbio/syaa013.
664 Zhao L, Li X, Zhang N, Zhang S-D, Yi T-S, Ma H, Guo Z-H, Li D-Z. 2016. Phylogenomic analyses of large-scale
665 nuclear genes provide new insights into the evolutionary relationships within the rosids. *Molecular*
666 *Phylogenetics and Evolution* 105:166-176 DOI: 10.1016/j.ympev.2016.06.007.
667 Zhao M-L, Song Y, Ni J, Yao X, Tan Y-H, Xu Z-F. 2018. Comparative chloroplast genomics and phylogenetics of
668 nine *Lindera* species (Lauraceae). *Scientific Reports* 8:8844 DOI: 10.1038/s41598-018-27090-0.
669

Table 1(on next page)

Sampled species and voucher specimens of Laureae in this study.

1

Taxon	Herbarium	Voucher	Geographic origin	GenBank Accession number
Actinodaphne obovata (Nees) Bl.	IBSC	XTBGLQM0236	Xishuangbanna, Yunnan, China	MN274947
Iteadaphne caudata (Nees) H. W. Li	IBSC	XTBGLQM0582	Xishuangbanna, Yunnan, China	MN428456
Lindera erythrocarpa Makino	IBSC	180923	Baishanzu Mountain, Zhejiang, China	MN428457
Litsea acutivena Hay.	\	\	Chebaling, Guangdong, China	MN428458
Litsea dilleniifolia P. Y. Pai et P. H. Huang	IBSC	XTBGLQM0095	Xishuangbanna, Yunnan, China	MN428459
Litsea elongata (Wall. ex Nees) Benth. et Hook. f.	IBSC	WBGQXJ001	Badagong Mountain, Hunan, China	MN428460
Litsea glutinosa (Lour.) C. B. Rob.	IBSC	XTBGLQM0653	Xishuangbanna, Yunnan, China	MN428461
Litsea mollis Hemsl.	IBSC	CFL2678	Libo county, Guizhou, China	MN428462
Litsea monopetala (Roxb.) Pers.	IBSC	XTBGLQM0687	Xishuangbanna, Yunnan, China	MN428463
Litsea pungens Hemsl.	IBSC	WBGQXJ124	Badagong Mountain, Hunan, China	MN428464
Litsea szemaois (H. Liu) J. Li et H.W. Li	IBSC	XTBGLQM0692	Xishuangbanna, Yunnan, China	MN428465
Neolitsea pallens (D. Don) Momiy. et H. Hara	IBSC	18371	Dinghu Mountain, Guangdong, China	MN428466

2

Table 2(on next page)

Summary of 12 complete plastomes of Laureae.

1

	Actinodaphne obovata	*Iteadaphne caudata*	*Lindera erythrocarpa*	*Litsea acutivena*	*Litsea elongata*	*Litsea glutinosa*
Total cpDNA size (bp)	152579	152863	152916	152718	152793	152748
Length of LSC region (bp)	93655	93761	93921	93677	93827	93698
Length of IR region (bp)	20057	20144	20071	20066	20066	20062
Length of SSC region (bp)	18810	18814	18853	18909	18844	18926
Total GC content (%)	39.1	39.1	39.1	39.2	39.1	39.2
LSC GC content (%)	37.9	38.0	37.9	38.0	37.9	38.0
IR GC content (%)	44.4	44.4	44.4	44.4	44.4	44.5
SSC GC content (%)	33.9	33.8	34.0	33.9	33.9	33.8
Total number of genes (unique)	127 (112)	127 (112)	127 (112)	127 (112)	127 (112)	127 (112)
Protein-coding genes (unique)	84 (78)	84 (78)	84 (78)	84 (78)	84 (78)	84 (78)
Total number of tRNA	36 (30)	36 (30)	36 (30)	36 (30)	36 (30)	36 (30)
Total number of rRNA	8 (4)	8 (4)	8 (4)	8 (4)	8 (4)	8 (4)

2

	Litsea dilleniifolia	*Litsea mollis*	*Litsea monopetala*	*Litsea pungens*	*Litsea szemaois*	*Neolitsea pallens*
Total cpDNA size (bp)	152298	152736	152705	152655	152132	152699
Length of LSC region (bp)	93218	93655	93758	93520	93119	93761
Length of IR region (bp)	20094	20063	20074	20131	20090	20071
Length of SSC region (bp)	18892	18936	18799	18873	18843	18796
Total GC content (%)	39.2	39.2	39.2	39.2	39.2	39.1
LSC GC content (%)	38.0	38.0	38.0	37.9	38.1	37.9
IR GC content (%)	44.4	44.4	44.4	44.4	44.4	44.4
SSC GC content (%)	34.0	33.9	33.9	34.0	34.0	33.9
Total number of genes (unique)	127 (112)	127 (112)	127 (112)	127 (112)	127 (112)	127 (112)
Protein-coding genes (unique)	84 (78)	84 (78)	84 (78)	84 (78)	84 (78)	84 (78)
Total number of tRNA	36 (30)	36 (30)	36 (30)	36 (30)	36 (30)	36 (30)
Total number of rRNA	8 (4)	8 (4)	8 (4)	8 (4)	8 (4)	8 (4)

3

Figure 1

Complete plastid genome map of Laureae.

Different functional genes are color coded. Genes outside the circle are transcribed counterclockwise, genes inside the circle are transcribed clockwise. GC content is indicated by darker gray in the inner circle.

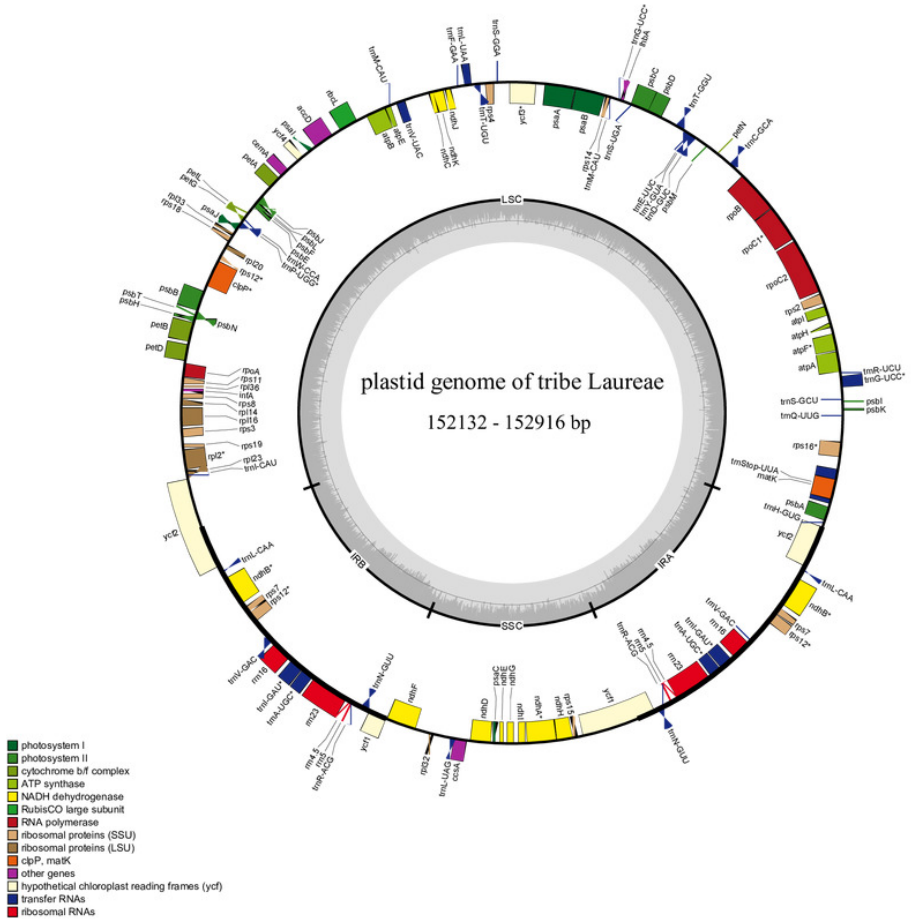
plastid genome of tribe Laureae
152132 - 152916 bp
LSC
IRB
IRA
SSC
photosystem I
photosystem II
cytochrome b/f complex
ATP synthase
NADH dehydrogenase
RubisCO large subunit
RNA polymerase
ribosomal proteins (SSU)
ribosomal proteins (LSU)
clpP, matK
other genes
hypothetical chloroplast reading frames (ycf)
transfer RNAs
ribosomal RNAs

Figure 2

Maximum likelihood phylogenetic tree of Laureae inferred with RAxML-NG based on complete plastomes.

Bootstrap values are indicated on branches. Subclades I, II and III are colored in red, green and blue, respectively.

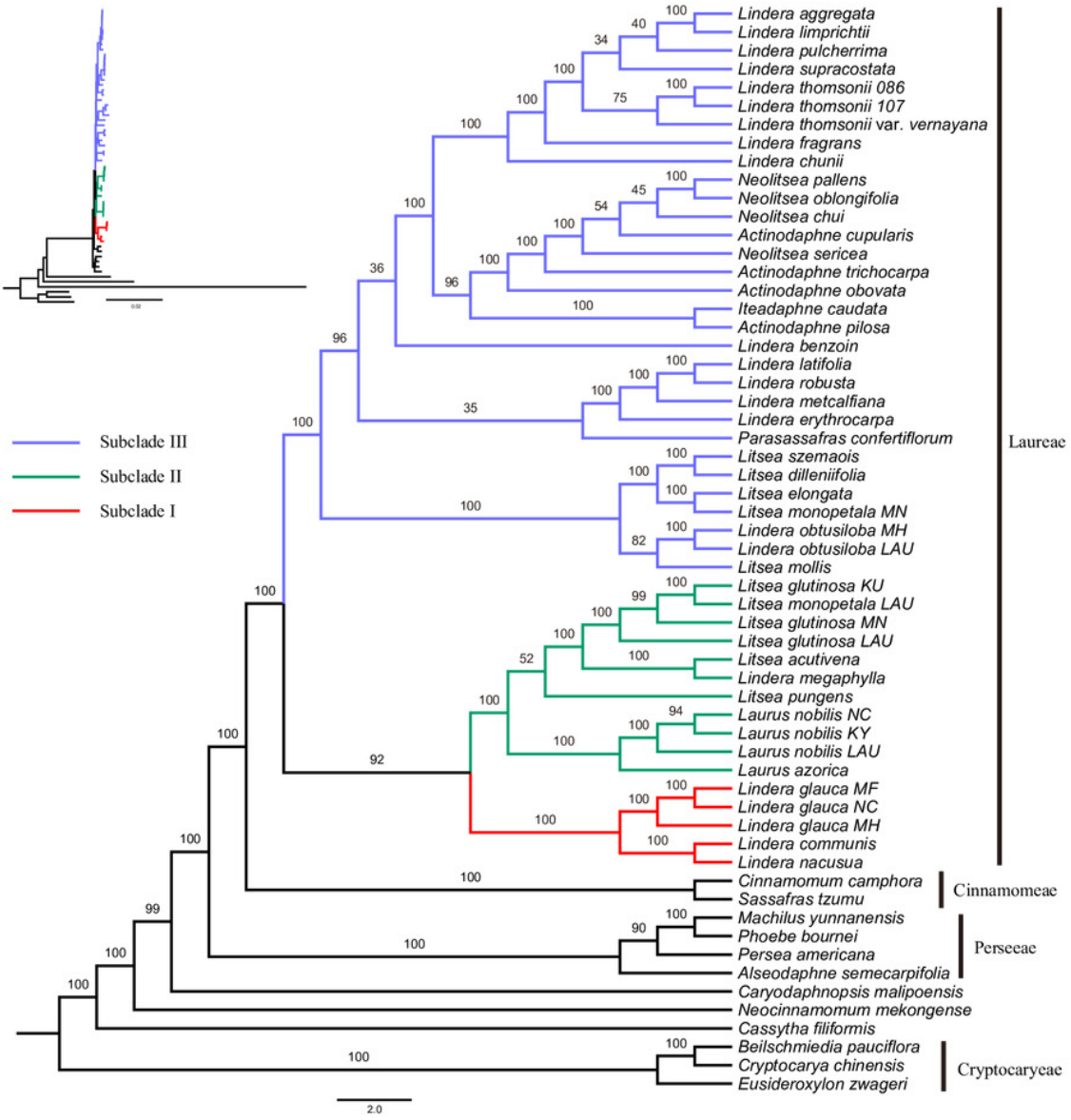
Subclade III
Subclade II
Subclade I
Lindera aggregata
Lindera limprichtii
Lindera pulcherrima
Lindera supracostata
Lindera thomsonii 086
Lindera thomsonii 107
Lindera thomsonii var. vernayana
Lindera fragrans
Lindera chunii
Neolitsea pallens
Neolitsea oblongifolia
Neolitsea chui
Actinodaphne cupularis
Neolitsea sericea
Actinodaphne trichocarpa
Actinodaphne obovata
Iteadaphne caudata
Actinodaphne pilosa
Lindera benzoin
Lindera latifolia
Lindera robusta
Lindera metcalfiana
Lindera erythrocarpa
Parasassafras confertiflorum
Litsea szemaois
Litsea dilleniifolia
Litsea elongata
Litsea monopetala MN
Lindera obtusiloba MH
Lindera obtusiloba LAU
Litsea mollis
Litsea glutinosa KU
Litsea monopetala LAU
Litsea glutinosa MN
Litsea glutinosa LAU
Litsea acutivena
Lindera megaphylla
Litsea pungens
Laurus nobilis NC
Laurus nobilis KY
Laurus nobilis LAU
Laurus azorica
Lindera glauca MF
Lindera glauca NC
Lindera glauca MH
Lindera communis
Lindera nacusua
Cinnamomum camphora
Sassafras tzumu
Machilus yunnanensis
Phoebe bournei
Persea americana
Alseodaphne semecarpifolia
Caryodaphnopsis malipoensis
Neocinnamomum mekongense
Cassytha filiformis
Beilschmiedia pauciflora
Cryptocarya chinensis
Eusideroxylon zwageri
Laureae
Cinnamomeae
Perseeae
Cryptocaryeae
2.0

Figure 3

Tree of Laureae inferred with ASTRAL III using a multispecies coalescent approach.

Local posterior probabilities (LPP) are indicated on branches. Subclades I, II and III are colored in red, green and blue, respectively.

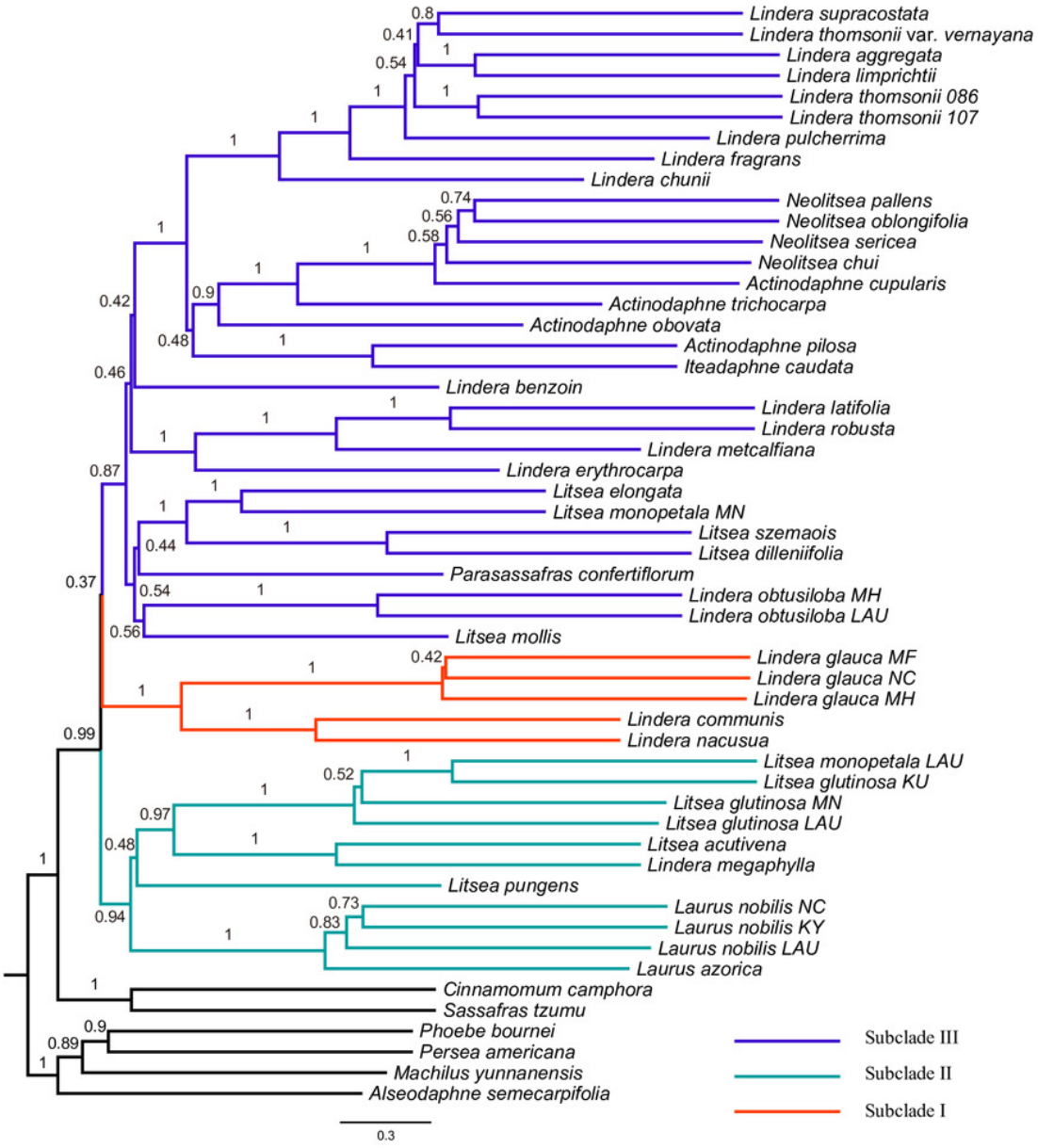
Lindera supracostata
Lindera thomsonii var. vernayana
Lindera aggregata
Lindera limprichtii
Lindera thomsonii 086
Lindera thomsonii 107
Lindera pulcherrima
Lindera fragrans
Lindera chunii
Neolitsea pallens
Neolitsea oblongifolia
Neolitsea sericea
Neolitsea chui
Actinodaphne cupularis
Actinodaphne trichocarpa
Actinodaphne obovata
Actinodaphne pilosa
Iteadaphne caudata
Lindera benzoin
Lindera latifolia
Lindera robusta
Lindera metcalfiana
Lindera erythrocarpa
Litsea elongata
Litsea monopetala MN
Litsea szemaois
Litsea dilleniifolia
Parasassafras confertiflorum
Lindera obtusiloba MH
Lindera obtusiloba LAU
Litsea mollis
Lindera glauca MF
Lindera glauca NC
Lindera glauca MH
Lindera communis
Lindera nacusua
Litsea monopetala LAU
Litsea glutinosa KU
Litsea glutinosa MN
Litsea glutinosa LAU
Litsea acutivena
Lindera megaphylla
Litsea pungens
Laurus nobilis NC
Laurus nobilis KY
Laurus nobilis LAU
Laurus azorica
Cinnamomum camphora
Sassafras tzumu
Phoebe bournei
Persea americana
Machilus yunnanensis
Alseodaphne semecarpifolia
Subclade III
Subclade II
Subclade I
0.3

Figure 4

Difference in the log-likelihood (lnL) of each plastid locus between two alternative topologies.

The x axis indicates each locus, and the y axis indicates lnL difference. (A) Positive and negative values support the topology showing subclades I-II (T1) and subclades II-III (T2), respectively. (B) Positive and negative values support the topology showing subclades I-II (T1) and subclades I-III (T3), respectively. (C) Positive and negative values support the topology showing subclades II-III (T2) and subclades I-III (T3), respectively. Values starting with + or – indicate the sum of positive and negative values, respectively, and the number of supporting loci is shown in the parenthesis. Note that the order of loci on x axis are different among A, B and C.

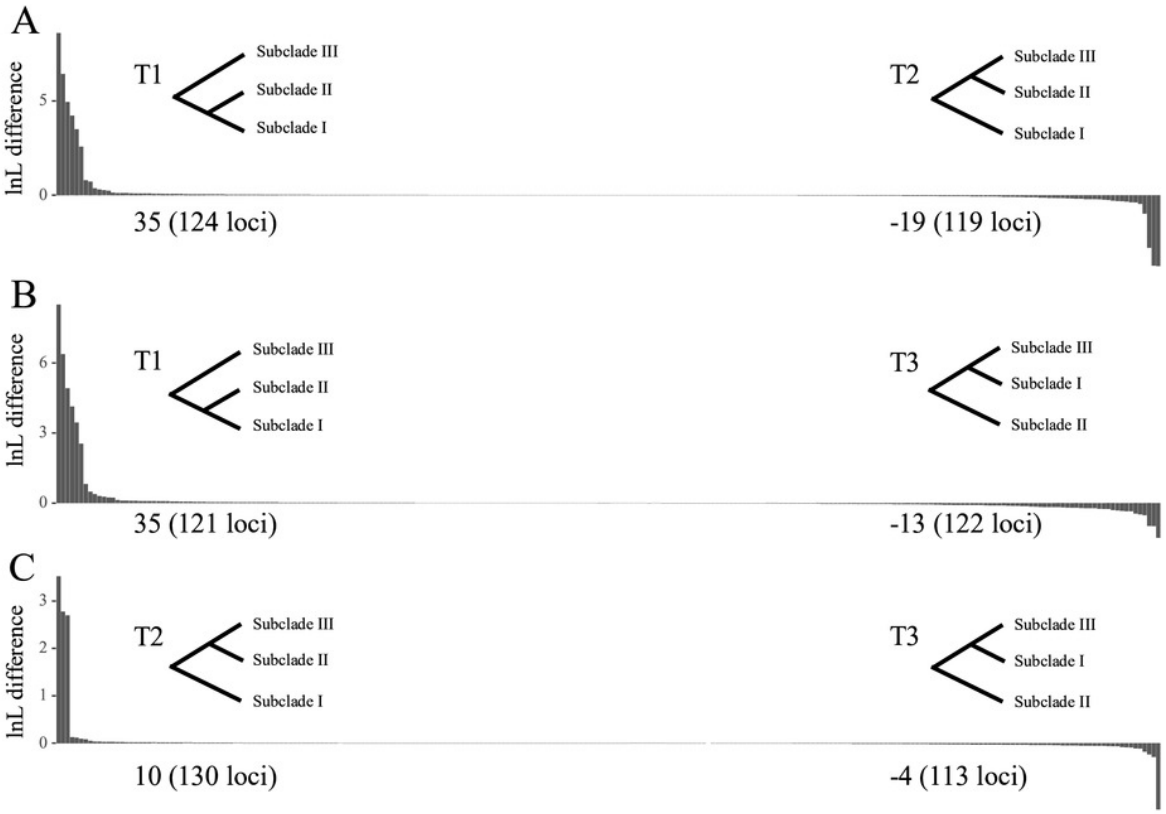
A
lnL difference
5
0
T1
Subclade III
Subclade II
Subclade I
T2
Subclade III
Subclade II
Subclade I
35 (124 loci)
-19 (119 loci)
B
lnL difference
6
3
0
T1
Subclade III
Subclade II
Subclade I
T3
Subclade III
Subclade I
Subclade II
35 (121 loci)
-13 (122 loci)
C
lnL difference
3
2
1
0
T2
Subclade III
Subclade II
Subclade I
T3
Subclade III
Subclade I
Subclade II
10 (130 loci)
-4 (113 loci)